ESC European Society of Cardiology

European Journal of Preventive Cardiology (2026) **00**, 1–16
https://doi.org/10.1093/eurjpc/zwag435

FULL RESEARCH PAPER
Imaging

Gene–environment interactions shape cytokine-mediated inflammation and cardiovascular risk

Mattia Corianò [1,2], Shamin Tahasildar [1], Ling Huang [1,3], Khaled Rjoob [1], Majid Vafaeezadeh [1], Soodeh Kalaie [1,3], Jin Zheng [1], Lara Curran [1,4,5], Parisa Gifani [1], Marc-Emmanuel Dumas [6,7,8], and Declan P O'Regan [1]*

[1]MRC Laboratory of Medical Sciences, Imperial College London, Hammersmith Hospital Campus, Du Cane Road, London W12 0HS, UK; [2]Department of Cardiac, Thoracic, Vascular Science and Public Health, University of Padova, Padova, Italy; [3]Department of Computing, Imperial College London, London, UK; [4]National Heart and Lung Institute, Imperial College London, London, UK; [5]Royal Brompton and Harefield Hospitals, Guy's and St. Thomas' NHS Foundation Trust, London, UK; [6]Division of Systems Medicine, Department of Metabolism, Digestion and Reproduction, Imperial College London, London, UK; [7]Multi-omics and Pathophysiology of Metabolic Disease Unit, Lille University Hospital, Lille, France; and [8]Antoine Lavoisier Multiscale Metabolism International Research Laboratory, Imperial College London, London, UK

Received 24 April 2026; revised 8 July 2026; accepted 17 August 2026; online publish-ahead-of-print 18 September 2026

Background Chronic inflammation is a major driver of cardiovascular diseases, but mechanisms linking systemic inflammation to cardiac remodelling remain incompletely understood. We aimed to evaluate the role of cytokine-mediated signalling and the influence of environmental and genetic factors on inflammation and cardiac phenotypes in a large population-based cohort.

Methods We analysed subsets of 488 079 UK Biobank participants with metabolomic and proteomic profiling, cardiac magnetic resonance (CMR) imaging, and longitudinal outcomes. Chronic inflammation was quantified using glycoprotein acetyls (GlycA) by nuclear magnetic resonance spectroscopy. Machine learning-based analysis extracted CMR phenotypes. Multivariable linear regression assessed GlycA-cardiac associations. Mediation analysis tested 80 inflammatory proteins as potential mediators. Cox models evaluated GlycA levels and major adverse cardiovascular events (MACEs). An exposome-wide association study identified environmental determinants of inflammation, and gene–environment interactions were assessed using multi-ancestry polygenic risk scores.

Results Higher GlycA levels were associated with reduced left ventricular indexed end-diastolic volume ($\beta = -2.09$) and stroke volume ($\beta = -1.12$), with compensatory increased heart rate ($\beta = 1.38$; all $P < 10^{-228}$). Interleukin (IL)-1 receptor antagonist statistically mediated 27% of the GlycA effect on end-diastolic volume (average causal mediated effect -0.53 [95% CI, -0.64 to -0.41]; $P < 10^{-16}$). The highest GlycA quintile had 43% higher MACE risk versus the lowest (adjusted HR, 1.43 [95% CI, 1.38–1.49]). Trunk fat mass ($\beta = 0.35$), current smoking ($\beta = 0.39$), psychological distress, and low socioeconomic status were the strongest GlycA determinants (all $P < 10^{-50}$). Cardiovascular polygenic risk scores modified associations between environmental exposures, inflammation, and MACE.

Conclusions Chronic systemic inflammation is associated with reduced left ventricular volumes and increased cardiovascular risk in the community, with circulating cytokines and growth factors including IL-1 and TNF identified as potential mediators of these associations. Exposure-gene interactions are associated with inflammatory responses such that risk may reflect the convergence of inherited and acquired factors.

Lay summary Long-term inflammation is linked to harmful changes in heart structure and function, and raises the risk of heart attack and stroke, even in people without known heart disease. We studied nearly 480 000 people, measuring

* Corresponding author. Tel: +44 2075945444, Email: declan.oregan@lms.mrc.ac.uk
© The Author(s) 2026. Published by Oxford University Press on behalf of the European Society of Cardiology.
This is an Open Access article distributed under the terms of the Creative Commons Attribution License (https://creativecommons.org/licenses/by/4.0/), which permits unrestricted reuse, distribution, and reproduction in any medium, provided the original work is properly cited.

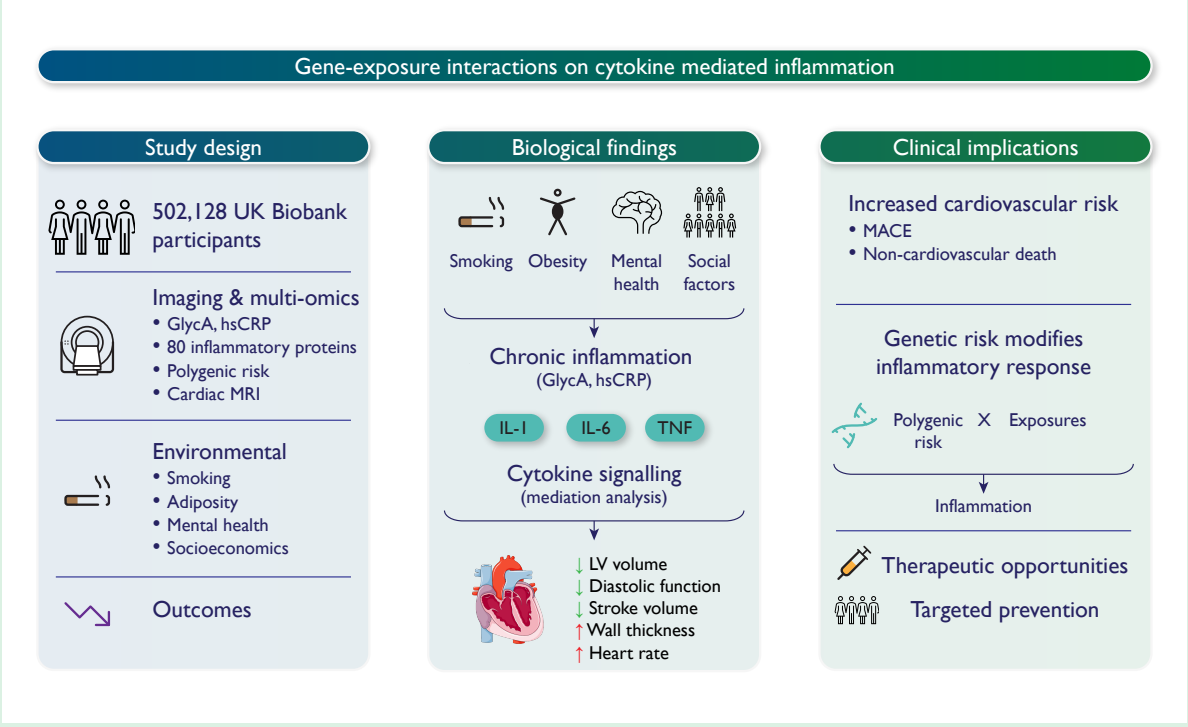
Downloaded from academic.oup.com/eurjpc/advance-article/doi/10.1093/eurjpc/zwag435/8802224 by Imperial College of Science Technology and Medicine user on 25 September 2026

inflammation using the blood marker glycoprotein acetyls (GlycA), combined with heart imaging and genetic data. People with higher chronic inflammation tend to have smaller heart chambers, thicker heart walls, and a heart that does not fill with blood efficiently–changes that can silently precede heart failure. Specific inflammatory proteins, particularly those in the interleukin-1 and TNF families, were identified as potential mediators of these harmful changes and are already being targeted by new drugs in clinical trials. We also found that a person's genes may influence how strongly their body reacts to stressors such as smoking, excess body fat, poor mental health, and deprivation, shaping both inflammation levels and heart disease risk. These findings suggest that chronic inflammation is a key link between everyday stressors and heart disease, and that combining inflammation markers with genetic risk could help identify people who would benefit most from early intervention.

Key findings

- Specific proteins in the interleukin-1 and TNF families may partly explain the association between inflammation, cardiac remodelling, and the risk of heart attack and stroke.
- A person's genes may influence how strongly their body responds to stressors like smoking, excess body fat, poor mental health, and poverty, modifying both inflammation levels and heart disease risk.

Graphical Abstract



The study included UK Biobank participants with metabolomic and proteomic profiling, CMR imaging, ECG, environmental exposures, body fat analysis, polygenic risk profiles and longitudinal outcomes. Chronic inflammation was quantified using GlycA by nuclear magnetic resonance spectroscopy. The association between systemic inflammation and cardiac remodelling was assessed in a subset of 70 809 participants considering 33 IDPs from CMR and 16 ECG traits. Mediation analysis tested 80 inflammatory proteins as potential mediators in 8184 individuals. Outcome analysis investigated the association of GlycA on MACE and all-cause death on top of lipid profile (454 821), IDPs (72 541), and considering proteins as mediators (48 427). An exposome-wide association study on 478 941 volunteers identified environmental determinants of inflammation, and gene–environment interactions were assessed using multi-ancestry polygenic risk scores available for 454 821 participants. GlycA, glycoprotein acetyls; hsCRP, high-sensitivity C-reactive protein; IL, interleukin; LV, left ventricle; MACEs, major adverse cardiac events; MRI, magnetic resonance imaging; TNF, tumor necrosis factor. Images provided by Servier Medical Art, licensed under CC BY 4.0.

Keywords Inflammation • Genetics • Environment • Heart • Cardiovascular magnetic resonance imaging

Downloaded from academic.oup.com/eurjpc/advance-article/doi/10.1093/eurjpc/zwag435/8802224 by Imperial College of Science Technology and Medicine user on 25 September 2026

Introduction

Chronic low-grade inflammation has emerged as a clinically actionable mediator of cardiovascular disease (CVD). Residual inflammatory risk, independent of traditional lipid-based factors, predicts adverse outcomes and represents a therapeutic target for both primary and secondary prevention.[1] There is also growing evidence that systemic inflammation is a hallmark of non-ischemic heart failure (HF), particularly when complicated by cardio-metabolic disease.[2,3] However, the interacting mechanisms triggering, regulating and responding to systemic inflammation in the adult population have not been addressed by previous biomarker outcome studies.[4,5,6] Consequently, neither inflammation-associated cardiac phenotypes nor the specific proteins mediating cardiac adaptation have been systematically characterized at population scale.

Equally important are the environmental and genetic determinants of chronic inflammation. While individual environmental exposures have been linked to inflammation and mortality,[7,8] and[9] we lack comprehensive exposome-wide analyses that identify key environmental drivers and their interaction with genetic susceptibility.[10] Given that combined assessments of clinical, metabolomic, and polygenic scores offer improved cardiovascular risk prediction,[11] discovering the causes, consequences, and modifiers of systemic inflammation is needed to support individualized prevention and the prioritization of new therapeutic strategies in diverse risk groups.

Taking advantage of large-scale assays of stable inflammatory biomarkers in deeply phenotyped populations with multi-omic profiling, we sought to determine the structural, proteomic, and environmental underpinnings of inflammatory risk. Using circulating glycoprotein acetyls (GlycA) as a stable and sensitive composite marker of chronic inflammation,[12] we characterized the predominant pattern of cardiac remodelling through machine learning analysis of cardiovascular imaging. To establish a comprehensive risk framework, we assessed the prognostic link between GlycA and major adverse cardiovascular events (MACEs) in the community, resolved the specific protein mediators of this association, and mapped the interaction between the exposome and multi-ancestry polygenic risk scores (PRS) in driving systemic inflammation. By defining the environmental, genetic, and phenotypic architecture of chronic inflammation, we aim to define the pathways linking chronic inflammation to cardiac remodelling and to identify potential targets for therapeutic prioritization in a risk-diverse population.

Methods

Study overview

The UK Biobank (UKB) study enrolled approximately 500 000 community-dwelling participants aged 40–69 years from across the United Kingdom, between 2006 and 2010.[13] All participants provided written informed consent, and the study received approval from the National Research Ethics Service (11/NW/0382). Our analysis was conducted under access approval number 40616, with data last accessed on December 1, 2025.

An overview of the study is shown in the *Graphical Abstract*. We used nuclear magnetic resonance (NMR) metabolomics data in 488 079 participants to quantify circulating GlycA.[14] Within this group, we assessed the relationship between GlycA and incident outcomes. To investigate the relationship between systemic inflammation and cardiac remodelling, we employed machine learning techniques to derive 33 imaging-derived phenotypes (IDPs) of cardiac structure and function from cardiac magnetic resonance (CMR) imaging and 16 electrocardiogram (ECG) traits in a subset of 70 809 participants.[15] This analysis enabled us to determine associations between GlycA levels and quantitative measures of cardiac morphology and function.

We further investigated the proteomic landscape underlying GlycA elevation by analysing 80 proteins, selected *a priori* based on their established roles in systemic inflammatory processes.[16] These proteins were assessed in 52 503 participants with available metabolomics and proteomics profiles. Each protein was evaluated both as a predictor of GlycA levels and as a potential mediator of associations between GlycA and cardiac IDPs or clinical outcomes. Mediation analysis was used to determine the proportion of GlycA's effect that was explained through each protein pathway.

To identify environmental determinants of systemic inflammation, we performed an exposome-wide association study (XWAS) in 478 941 participants, examining 169 environmental exposures and 8 body composition measurements in relation to GlycA levels.[7] Exposures demonstrating significant associations with inflammation were subsequently analysed for interactions with 10 multi-ancestry cardiovascular disease PRSs. Gene–environment interactions were tested using interaction terms in multivariable linear regression models for GlycA levels and Cox proportional hazards models for MACEs.

Blood biomarkers

UKB provides measurements of a comprehensive range of biochemical markers from biological samples collected at baseline (2006–10) across all 500 000 participants. For this study, we analysed variables from the biochemistry, metabolite, and proteomic biomarker panels.

Biochemistry biomarkers were obtained from 473 133 participants at baseline recruitment. Technical details of quantitative analyses have been previously described.[17] We analysed the following biochemistry biomarkers: creatinine (field ID 30700), HbA1c (field ID 30750), high-sensitivity C-reactive protein (hsCRP) (field ID 30710), and lipoprotein(a) [Lp(a)] (field ID 30790).

NMR metabolomics measures were obtained from 488 079 participants recruited at baseline and profiled by Nightingale Health. Technical details of the quantitative serum NMR analysis have been previously described.[18] Pre-processing included removal of technical variation, recalculation of derived biomarkers, removal of outlier values, normal distribution transformation, and standardization as described in the Supplementary Methods. For this study, we considered GlycA (field ID 23480) as a marker of chronic inflammation. Data from the November 2025 release were used in this study.

Proteomic profiling was obtained from 53 013 participants recruited at baseline and performed using the Olink Explore 3072 platform, which integrates four Olink panels (Cardiometabolic, Inflammation, Neurology, and Oncology). UKB Olink data are provided as normalized protein expression values on a log2 scale. For the present study, we focused on 80 biomarkers from the Olink Inflammation panel (Supplementary material online, *Table S1*).[16]

Cardiovascular imaging analysis

CMR imaging was performed on a 1.5T scanner (MAGNETOM Aera, Siemens Healthineers, Erlangen, Germany) using retrospectively gated balanced steady-state free precession cine sequences.[19] Left ventricle (LV) short-axis cine images were acquired from base to apex, along with long-axis cine images in the two-chamber and

Downloaded from academic.oup.com/eurjpc/advance-article/doi/10.1093/eurjpc/zwag435/8802224 by Imperial College of Science Technology and Medicine user on 25 September 2026

four-chamber planes. Cines comprised 50 cardiac phases with a typical temporal resolution of 31 ms. Transverse cine images of the ascending and descending thoracic aorta were also acquired.

Images were segmented using fully convolutional neural networks previously validated in the UKB,[20] with segmentation quality equivalent to expert human readers, as described in the Supplementary Methods.

Derived measurements of the left and right ventricles were determined from the two-dimensional images: indexed end-diastolic volume (EDVi), indexed end-systolic volume (ESVi), stroke volume, and ejection fraction (EF). LV mass was calculated from myocardial volume using an assumed myocardial density of 1.05 g/mL. Atrial volumes were derived using the biplane area-length method: $V = \frac{8}{3\pi} \cdot \frac{A_{2Ch} \cdot A_{4Ch}}{L}$, where A_{2Ch} and A_{4Ch} represent the atrial areas on the two-chamber and four-chamber views, respectively, and L is the averaged longitudinal diameter across the two views. CMR-derived measurements were indexed to body surface area (BSA) calculated using the Du Bois formula: BSA = $0.007184 \cdot \text{Height}^{0.725} \cdot \text{Weight}^{0.425}$, with height in cm and weight in kg. LV wall thickness was measured as the distance between the segmented epicardium and endocardium at end-diastole.

Myocardial strain analysis was performed using non-rigid free-form deformation image registration between successive frames.[21] To reduce accumulation of registration errors, motion tracking was performed in both forward and backward directions from the end-diastolic frame, and an average displacement field was calculated.[22] Circumferential (E_{cc}) and radial (E_{rr}) strains were calculated using short-axis cines as $E_{dir} = \frac{\Delta L_{dir}}{L_{dir}}$, where *dir* represents the circumferential or radial direction, L_{dir} is the absolute length of a line segment along this direction, and ΔL_{dir} is its change in length over time. Longitudinal (E_{ll}) strain was calculated from long-axis four-chamber motion tracking. Strain rate was estimated as the first derivative of strain, and peak-diastolic strain rate (PDSR) in the radial and longitudinal directions was detected using an algorithm to identify local maxima.[22]

A spatio-temporal neural network was used to segment the aortic cine images.[15] Maximum and minimum cross-sectional areas were derived, and aortic distensibility was calculated using central blood pressure obtained from peripheral pulse-wave analysis (Vicorder, SMT Medical, Würzburg, Germany).[23]

A total of 33 IDPs characterizing cardiac volumes and function, as well as vascular stiffness, were extracted.

Electrocardiogram

Twelve-lead ECG recordings were obtained from UKB participants using a standardized acquisition protocol and analysed with proprietary software (GE CardioSoft). Raw 15-second, 12-lead ECG signals from 81 964 participants were processed through a validated computational pipeline to systematically extract quantitative ECG biomarkers. This analysis yielded 16 distinct ECG parameters for subsequent cardiovascular risk assessment.

Environmental factors

We assessed the impact of environmental exposures on systemic inflammation using the analytical framework developed by Argentieri *et al.*[7] From 176 baseline exposure variables available as of August 1, 2025, we retained variables with less than 45% missing data that were consistently collected across all assessment centers. This yielded 148 candidate exposures for analysis.

Prior to analysis, all continuous variables were centered and standardized, with the exception of age at recruitment. Ordinal categorical variables were recoded to enable linear association testing, while nominal categorical exposures were analysed using the most frequent category as the reference group. Multi-select ('mark all that apply') responses were converted to binary dummy variables to facilitate statistical modelling.

The final analytical dataset exhibited an average missing data rate of 6% across all variables (range: 0–44%). We addressed missing values using the R package `missRanger`, which employs random forest imputation combined with predictive mean matching. Imputation parameters included a maximum of 10 iterations, 200 trees per random forest, and 16 processing threads, with remaining hyperparameters using default settings. Following imputation and variable recoding, 169 environmental exposures were available for XWAS analysis.

Comprehensive data dictionaries detailing all XWAS exposures are provided in Supplementary material online, *Table S2*, with variable recoding procedures described in the Supplementary Methods.

Body composition

Abdominal and whole-body adipose tissue assessment was performed using 1.5T dual-echo Dixon Vibe imaging from neck to knees. Six overlapping sections underwent calibration, stacking, fusion, and segmentation using AMRA Researcher software (AMRA Medical AB, Linköping, Sweden). Android and gynoid adipose tissue masses were quantified using self-supervised, multi-modal alignment between magnetic resonance imaging and dual-energy X-ray absorptiometry scans.[24] Liver proton density fat fraction was measured using the least median of squares Dixon method during single breath-hold acquisitions.[25] For this study, we considered eight body fat composition measurements reflecting total fat and specific adiposity patterns, as shown in Supplementary material online, *Table S3*.

Exposome-wide association study

XWAS analyses were performed using multivariable linear regression with log-transformed and scaled GlycA as the outcome variable, regressed against 177 factors (169 environmental exposures + 8 body composition measurements). Each model was adjusted for BSA, sex, age, age^2, age:sex interaction, and ethnicity (White, Asian, Black, or other). All continuous exposure variables were scaled and centered prior to analysis.

Analyses were conducted for the entire cohort (pooled cohort) and independently in each sex. Parallel XWAS analyses were performed using hsCRP as the outcome variable instead of GlycA.

P values were corrected for multiple testing using the false discovery rate (FDR) method (Benjamini–Hochberg procedure[26]) with a significance threshold of FDR $P < 0.05$.

Outcome data

UKB provides comprehensive health outcome information from multiple linked data sources. In this study, health outcomes were ascertained from self-reported medical history (field IDs 20002, 20008), inpatient hospital records (field IDs 41270 and 41280 for ICD-10 codes; 41271 and 41281 for ICD-9 codes; 20010 for operation codes), first occurrence datasets, and national death registries. The primary endpoint was the first occurrence of MACE, defined as a composite of cardiac arrest, HF, stroke or other cerebrovascular events, myocardial infarction, or cardiovascular death (Supplementary material online, *Table S4*). All-cause mortality was investigated as a secondary endpoint. Follow-up commenced at enrollment and continued until the first occurrence of MACE or death for metabolomics analyses, or from CMR acquisition until MACE or death for imaging-based analyses, depending on the specific research question.

Gene–environment interactions

We investigated gene–environment interactions using multi-ancestry PRSs for all-cause CVD, serum lipid levels, diabetes, hypertension, and stroke (Supplementary material online, *Table S5*). Details regarding

Downloaded from academic.oup.com/eurjpc/advance-article/doi/10.1093/eurjpc/zwag435/8802224 by Imperial College of Science Technology and Medicine user on 25 September 2026

the derivation of these PRS have been previously described.[27] We examined whether interactions between environmental factors and each PRS influence GlycA levels using multivariable linear regression models, and incident MACE using Cox proportional hazards models, as described in the Supplementary Methods. A secondary sensitivity analysis further adjusted for Townsend deprivation index at recruitment (field ID 22189) was performed. The Benjamini–Hochberg method was applied to control the false discovery rate by adjusting the *P*-values for multiple comparisons.[26]

Statistical analysis

Detailed statistical methods are provided in the Supplementary Methods. All analyses were performed using R version 4.5.0 and Python version 3.9.

Continuous variables are presented as mean ± standard deviation for normally distributed data or median (interquartile range [IQR]) for skewed distributions, and were compared using one-way analysis of variance or Kruskal–Wallis tests, respectively. Categorical variables are expressed as frequencies (percentages) and compared using χ^2 tests.

Associations between log-transformed and scaled GlycA and CMR-derived IDPs or ECG parameters were examined using multivariable linear regression models adjusted for potential confounders. Protein–GlycA associations were analysed using the same approach. Mediation analyses investigated each protein as a potential mediator of GlycA–IDP associations. Specifically, we used the `mediation` package in R, considering each IDP as the outcome variable, log-transformed and scaled GlycA as predictor, and proteins as mediators, and adjusted for potential confounders. Results are reported as average causal mediation effect (ACME), representing the average change in the outcome if the treatment were maintained constant but the mediator were altered, and mediated proportions, representing the ratio of ACME to the total effect, with 95% confidence interval (CI).

For survival analyses, participants were stratified by log-transformed and scaled GlycA quintiles (Q1, lowest; Q5, highest). Cox proportional hazards models were used to test GlycA as an independent predictor of primary and secondary endpoints beyond CMR features or lipid profiles, with adjustment for potential confounders. Sensitivity analyses employed Fine–Gray subdistribution hazards regression with non-cardiovascular death as a competing risk. Non-linear associations were explored using restricted cubic splines. Results are reported as hazard ratio (HR) with 95% CI. Mediation analyses examined proteins as potential mediators of GlycA–incident MACE associations using parametric survival models with Weibull distribution, adjusted for confounders and lipid profiles.

Given that hsCRP represents the most widely studied inflammatory biomarker, parallel analyses were conducted substituting log-transformed and scaled hsCRP for GlycA. To evaluate whether GlycA confers incremental prognostic value, a competing risk model was constructed including cardiovascular risk factors and hsCRP as predictors, and subsequently refitted with log-transformed and scaled GlycA added as an additional covariate. Model fit was assessed using likelihood ratio χ^2 tests, and net reclassification improvement (NRI) was calculated to evaluate the incremental predictive value for 10-year risk of MACE.

Statistical significance was defined as $P < 0.05$ (two-sided). Multiple comparison correction was performed using the Benjamini–Hochberg false discovery rate method.[26]

Results

Study cohort

A total of 502 128 participants aged 40–69 years were enrolled across the United Kingdom between 2006 and 2010. Of these, 189 individuals were excluded due to withdrawn consent, leaving 501 939 participants eligible for analysis.

Of the 501 939 participants with GlycA measurements, 488 079 individuals remained after metabolomic data preprocessing. The effect of chronic inflammation on cardiac remodelling was evaluated in participants with both CMR ($n = 81\,313$) and ECG ($n = 81\,964$) data, yielding 70 809 individuals with complete GlycA, CMR, and ECG measurements. Protein mediation analyses examining the interaction between GlycA and IDPs, as well as between GlycA and MACE, were conducted in 8184 and 48 427 participants with available proteomic data, respectively.

For survival analyses, participants with MACE occurring before CMR imaging ($n = 45\,733$) were excluded when testing inflammation effects on outcomes adjusted for IDPs, whereas those with MACE before enrollment ($n = 19\,131$) were excluded when testing inflammation effects adjusted for lipid profiles. This resulted in 72 541 and 454 821 individuals for CMR-adjusted and lipid-adjusted analyses, respectively.

For XWAS analyses, environmental exposure data were available for 492 110 individuals. After excluding 13 169 participants with incomplete data, 478 941 individuals had complete GlycA and environmental exposure measurements. Sample sizes for body composition analyses were detailed above.

Gene–environment interactions were investigated using 10 multi-ancestry PRSs for cardiovascular disease, which were available for 485 717 individuals.

Inflammation-driven cardiac remodelling

Baseline characteristics of participants with available metabolomic data are shown in Table 1. The majority of participants were women (54%) and of self-reported White ethnicity (95%). At recruitment, mean age was 57 ± 8 years, with 27% having hypertension, 10% being current smokers, 5.3% having diabetes, and 7% having previous MACE. Mean GlycA concentration was 0.82 ± 0.12 mmol/L for both sexes, and significantly differed among ethnicities, with Afro-Caribbean individuals showing the lowest value (all $P < 0.001$). Supplementary material online, *Table S6* shows demographic characteristics and IDPs stratified by GlycA quintiles. Body mass index, age, and blood pressure increased progressively across quintiles ($P < 0.001$ for all) (Supplementary material online, *Figure S1*).

After adjusting for confounders, higher GlycA was associated with reduced volumes across all cardiac chambers, for example LV EDVi ($\beta = -2.09$, $P < 10^{-200}$) (Figure 1A), as well as increased global LV wall thickness, reduced indexed LV mass ($\beta = -0.30$, $P < 10^{-20}$), and reduced diastolic function (longitudinal PDSR: $\beta = -0.04$, $P < 10^{-90}$). Furthermore, higher GlycA was associated with reduced stroke volume and increased heart rate ($\beta = 1.38$, $P < 10^{-200}$), but a negligible effect on cardiac index ($\beta < 0.01$) (Supplementary material online, *File 1*).

Findings were consistent across sex-stratified analyses (Figure 1B; Supplementary material online, *Files 2–3*), diabetes status ($r = 0.985$, $P = 3.1 \times 10^{-37}$; Supplementary material online, *Figure S2A*; Supplementary material online, *Files 4–5*), obesity status ($r = 0.993$, $P = 8.7 \times 10^{-46}$; Supplementary material online, *Figure S2B*; Supplementary material online, *Files 6–7*), and age groups (Supplementary material online, *Files 8–10*). Associations persisted after adjusting for hsCRP (Supplementary material online, *File 11*).

Downloaded from academic.oup.com/eurjpc/advance-article/doi/10.1093/eurjpc/zwag435/8802224 by Imperial College of Science Technology and Medicine user on 25 September 2026

Table 1. Baseline characteristics. Demographic, risk factors and blood biomarker among participants with available metabolomic data

Variable	Overall N = 488 079	Women N = 264 777	Men N = 223 302
Baseline characteristics			
Assessment centre			
England/Wales	453 522 (93%)	245 613 (93%)	207 909 (93%)
Scotland	34 557 (7.1%)	19 164 (7.2%)	15 393 (6.9%)
Age, years	57 ± 8	56 ± 8	57 ± 8
Ethnicity			
White	459 929 (95%)	249 786 (95%)	210 143 (95%)
Afro-Caribbean	8649 (1.8%)	5021 (1.9%)	3628 (1.6%)
Asian	11 786 (2.4%)	5782 (2.2%)	6004 (2.7%)
Other	5410 (1.1%)	3131 (1.2%)	2279 (1.0%)
BSA, m^2	1.90 ± 0.22	1.79 ± 0.18	2.04 ± 0.19
Household income			
<£18 000	102 336 (24%)	59 628 (26%)	42 708 (21%)
£18 000–£30 999	111 241 (26%)	61 518 (27%)	49 723 (25%)
£31 000–£51 999	109 637 (25%)	56 593 (25%)	53 044 (26%)
£52 000–£100 000	85 923 (20%)	42 141 (18%)	43 782 (22%)
>£100 000	22 644 (5.2%)	10 667 (4.6%)	11 977 (6.0%)
Townsend deprivation index	−1.32 ± 3.08	−1.35 ± 3.03	−1.29 ± 3.13
Smoking status			
Never	261 855 (55%)	154 758 (60%)	107 097 (49%)
Current	49 809 (10%)	22 926 (8.8%)	26 883 (12%)
Previous	165 496 (35%)	81 496 (31%)	84 000 (39%)
Hypercholesterolemia	74 393 (15%)	31 365 (12%)	43 028 (19%)
Hypertension	132 351 (27%)	62 292 (24%)	70 059 (31%)
Obesity	13 117 (2.7%)	7177 (2.7%)	5940 (2.7%)
Diabetes	25 716 (5.3%)	9725 (3.7%)	15 991 (7.2%)
Chronic kidney disease	6798 (1.4%)	3407 (1.3%)	3391 (1.5%)
Lowering cholesterol medication	75 809 (16%)	29 428 (11%)	46 381 (21%)
Previous heart failure	2669 (0.5%)	666 (0.3%)	2003 (0.9%)
Previous myocardial infarction	20 917 (4.3%)	6171 (2.3%)	14 746 (6.6%)
Previous MACE	33 258 (6.8%)	11 045 (4.2%)	22 213 (9.9%)
Blood biomarkers			
GlycA, mmol/L	0.82 ± 0.12	0.82 ± 0.12	0.82 ± 0.12
CRP, mg/L	1.33 (0.66, 2.76)	1.38 (0.65, 2.97)	1.28 (0.66, 2.54)
Lp(a), nmol/L	21 (10, 62)	22 (10, 62)	20 (9, 62)
HbA1c, mmol/mol	35.2 (32.8, 37.9)	35.2 (32.7, 37.7)	35.3 (32.8, 38.1)
Creatinine, μmol/L	70 (61, 81)	63 (57, 70)	80 (73, 88)
Total cholesterol, mmol/L	4.70 ± 0.96	4.90 ± 0.93	4.45 ± 0.92
Remnant cholesterol, mmol/L	1.58 ± 0.42	1.62 ± 0.43	1.5 ± 0.41
VLDL cholesterol, mmol/L	0.73 ± 0.25	0.72 ± 0.26	0.74 ± 0.24
LDL cholesterol, mmol/L	1.78 ± 0.45	1.81 ± 0.45	1.74 ± 0.45
HDL cholesterol, mmol/L	1.34 ± 0.34	1.47 ± 0.33	1.18 ± 0.27
Total triglycerides, mmol/L	1.22 (0.89, 1.68)	1.11 (0.82, 1.52)	1.37 (1.00, 1.83)

We next investigated the role of 80 inflammatory proteins in cardiac remodelling in 8184 participants with available CMR, proteomics, and metabolomics data. First, we identified proteins significantly associated with inflammatory biomarkers (both GlycA and hsCRP), as reported in Supplementary material online, *Figure S3* and Supplementary material online, *Files 12–13*. Second, we assessed whether these proteins mediate the association between GlycA and cardiac remodelling. As shown in Figure 2A, numerous proteins statistically mediated effects on LV and right ventricle (RV) EDVi, ESVi, and atrial volumes, predominantly involving tumor necrosis factor (TNF), transforming growth factor, interleukin (IL)-1,

Downloaded from academic.oup.com/eurjpc/advance-article/doi/10.1093/eurjpc/zwag435/8802224 by Imperial College of Science Technology and Medicine user on 25 September 2026

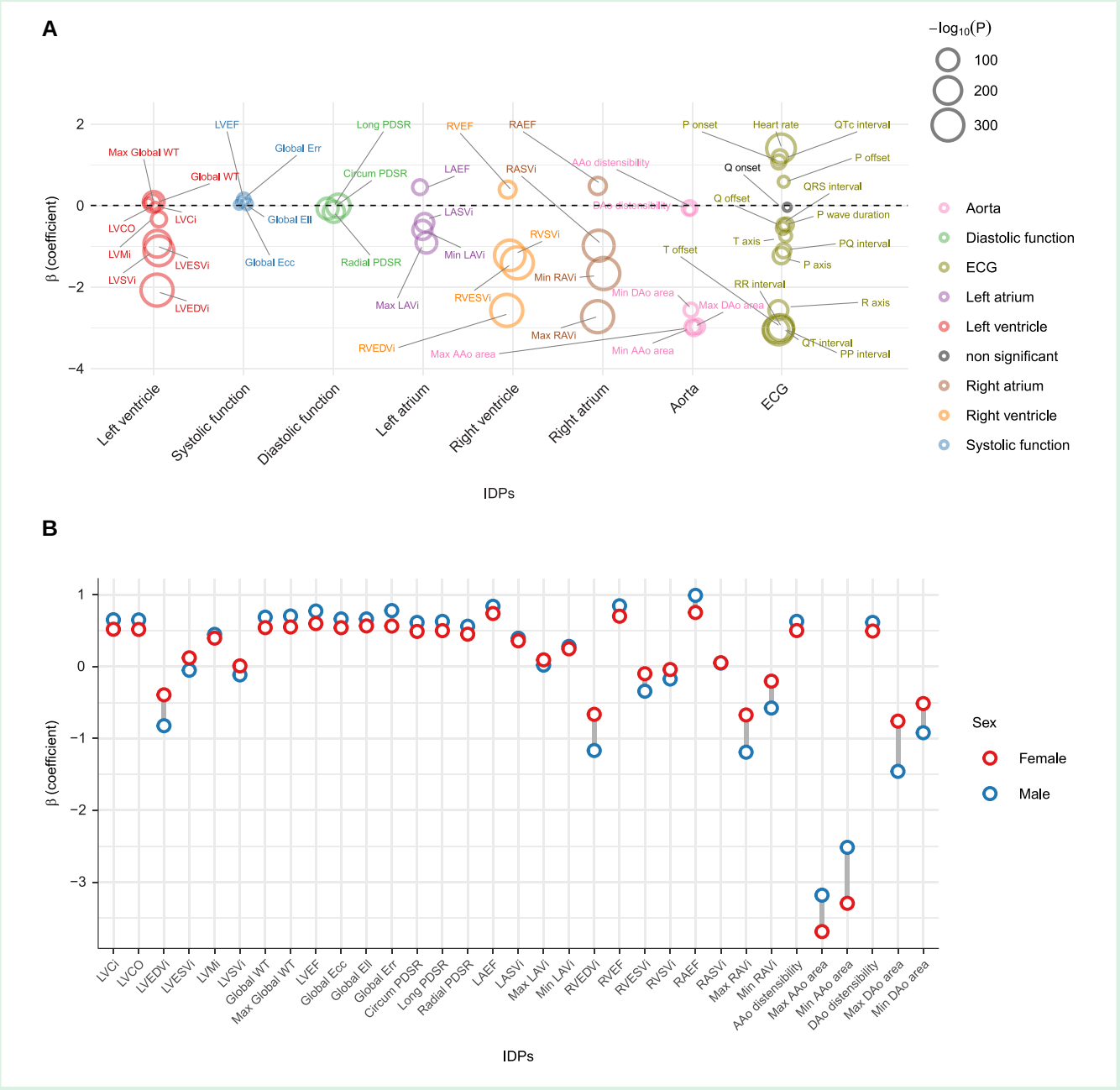


Figure 1. Effect of chronic inflammation on cardiac geometry. *(A)* Multivariable linear regression coefficients for the effect of GlycA on IDPs and ECG variables in the pooled cohort. Each IDP or ECG variable is considered as predictor, and regressed against log-transformed and scaled GlycA after adjusting for BSA, age at the date of CMR, sex, age:sex interaction, age^2, and diabetes status. β coefficients are scaled and a minimum cap of -3 is set for clarity; horizontal and vertical jitters are added to reduce points overlap. *(B)* Multivariable linear regression coefficients for the effect of GlycA on IDPs stratified by sex. β coefficients are scaled. AAo, ascending aorta; BSA, body surface area; CMR, cardiac magnetic resonance; DAo, descending aorta; DBP, diastolic blood pressure; ECG, electrocardiogram; EDVi, end-diastolic volume indexed; Ell, longitudinal strain; Ecc, circumferential strain; Err, radial strain; ESVi, end-systolic volume indexed; GlycA, glycoprotein acetyl; IDP, imaging-derived phenotype; LA, left atrium; LAEF, left atrial ejection fraction; LASVi, left atrial stroke volume indexed; LAVmax, maximum left atrial volume indexed; LAVmin, minimum left atrial volume indexed; LV, left ventricle; LVCO, left ventricular cardiac output; LVCi, left ventricular cardiac index; LVEDVi, left ventricular end-diastolic volume indexed; LVEF, left ventricular ejection fraction; LVESVi, left ventricular end-systolic volume indexed; LVMi, left ventricular mass indexed; LVSVi, left ventricular stroke volume indexed; MAP, mean arterial pressure; PDSR, peak diastolic strain rate; P, P wave; Q, Q wave; QRS, QRS interval; R, R wave; RA, right atrium; RAEF, right atrial ejection fraction; RASVi, right atrial stroke volume indexed; RAVmax, maximum right atrial volume indexed; RAVmin, minimum right atrial volume indexed; RV, right ventricle; RVEDVi, right ventricular end-diastolic volume indexed; RVEF, right ventricular ejection fraction; RVESVi, right ventricular end-systolic volume indexed; RVSVi, right ventricular stroke volume indexed; SBP, systolic blood pressure; SVi, stroke volume indexed; T, T wave; WT, LV myocardial wall thickness

Downloaded from academic.oup.com/eurjpc/advance-article/doi/10.1093/eurjpc/zwag435/8802224 by Imperial College of Science Technology and Medicine user on 25 September 2026

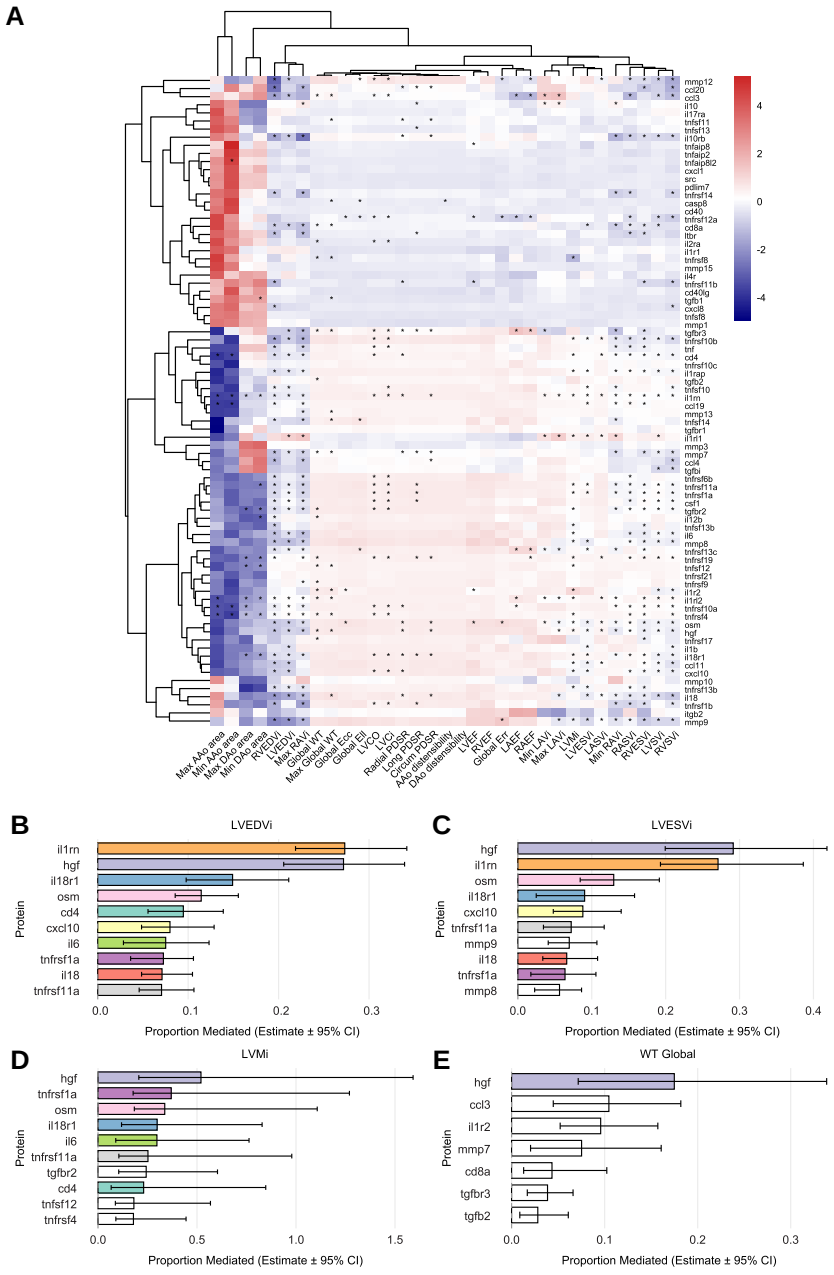


Figure 2. Proteins mediating the effect of inflammation on cardiac geometry. *(A)* Heatmap showing the scaled coefficients for the average causal mediation effect of each protein on each IDP. Each model included log-transformed and scaled GlycA as the exposure, one protein as the mediator, and one IDP as the outcome. Negative values indicate mediation of an association with lower IDPs value. Models were adjusted for BSA, sex, age, age^2, the age–sex interaction, and prevalent diabetes. (*) denotes an FDR-adjusted *p*-value <0.05. The bottom panel reports the proportion of the mediated effect for the top 10 proteins for LVEDVi *(B)*, LVESVi *(C)*, LVMi *(D)*, and global WT *(E)*. The proportion mediated effect represents the percentage of the total association between GlycA and incident MACE that is statistically mediated through each protein. AAo, ascending aorta; BSA, body surface area; DAo, descending aorta; EDVi, end-diastolic volume indexed; Ell, longitudinal strain; Ecc, circumferential strain; Err, radial strain; ESVi, end-systolic volume indexed; GlycA, glycoprotein acetyl; IDP, imaging-derived phenotype; LA, left atrium; LAEF, left atrial ejection fraction; LASVi, left atrial stroke volume indexed; LAVmax, maximum left atrial volume indexed; LAVmin, minimum left atrial volume indexed; LV, left ventricle; LVCO, left ventricular cardiac output; LVCi, left ventricular cardiac index; LVEDVi, left ventricular end-diastolic volume indexed; LVEF, left ventricular ejection fraction; LVESVi, left ventricular end-systolic volume indexed; LVMi, left ventricular mass indexed; LVSVi, left ventricular stroke volume indexed; MAP, mean arterial pressure; PDSR, peak diastolic strain rate; RA, right atrium; RAEF, right atrial ejection fraction; RASVi, right atrial stroke volume indexed; RAVmax, maximum right atrial volume indexed; RAVmin, minimum right atrial volume indexed; RV, right ventricle; RVEDVi, right ventricular end-diastolic volume indexed; RVEF, right ventricular ejection fraction; RVESVi, right ventricular end-systolic volume indexed; RVSVi, right ventricular stroke volume indexed; SVi, stroke volume indexed; WT, LV myocardial wall thickness

Downloaded from academic.oup.com/eurjpc/advance-article/doi/10.1093/eurjpc/zwag435/8802224 by Imperial College of Science Technology and Medicine user on 25 September 2026

and IL-6 signalling pathways. Figure 2B–E illustrates the proportion of mediated effect for four IDPs reflecting LV geometry.

Interleukin-1 receptor antagonist protein (IL-1RA) statistically mediated the largest proportion of the GlycA effect on LV EDVi (ACME −0.53 [95% CI: −0.64 to −0.41, $P < 10^{-16}$], proportion mediated 0.27 [95% CI: 0.22–0.34, $P < 10^{-16}$]) and demonstrated the strongest ACME on indexed LV mass (−0.18 [95% CI: −0.24 to −0.11, $P < 10^{-16}$]). Hepatocyte growth factor (HGF) statistically mediated the largest proportion of the GlycA effect on LV ESVi (ACME −0.26 [95% CI: −0.33 to −0.18, $P < 10^{-16}$], proportion mediated 0.29 [95% CI: 0.20–0.42, $P < 10^{-16}$]) and LV global wall thickness (ACME 0.01 [95% CI: 0.01 to 0.02, $P < 10^{-16}$], proportion mediated 0.17 [95% CI: 0.06–0.34, $P < 10^{-16}$]).

Extended data are provided in Supplementary material online, *File 14*. Mediation analyses for hsCRP effects on IDPs yielded comparable results (Supplementary material online, *Figure S4* and Supplementary material online, *File 15*).

Outcome analysis

After a median follow-up of 15.3 (14.3–16.0) years (17 777 person-years), 74 336 individuals experienced the primary endpoint. The majority of MACE events were myocardial infarction (7.7%), followed by stroke (6.6%) and HF (4.3%). For the secondary endpoint, 55 076 (11%) all-cause deaths were observed, including 10 377 cardiovascular deaths (Supplementary material online, *Table S7*).

Covariate-, lipid-, and competing risk-adjusted cumulative incidence curves for the probability of incident MACE and all-cause death rose with each quintile of GlycA (Figure 3, Supplementary material online, *Table S8*). The HR for the primary endpoint comparing quintile 5 with quintile 1 was 1.42 (1.38–1.49) for the competing risk model, declining to 1.09–1.18 after adjusting for hsCRP. GlycA remained an independent predictor of the primary endpoint after adjustment for IDPs and showed a non-linear association with MACE, with risk remaining stable at lower levels and increasing markedly above the median ($P < 0.001$ for non-linearity; Supplementary material online, *Figure S5*).

Similar results were found using log-transformed and scaled hsCRP instead of GlycA (Supplementary material online, *Table S9*), and when considering all-cause death as the outcome variable (Supplementary material online, *Table S10*). The addition of GlycA significantly improved predictive performance (log-likelihood ratio $\Delta\chi^2 P < 10^{-10}$) to a model fitted with hsCRP and cardiovascular risk factors for 10-year risk of MACE, as reported in Supplementary material online, *Table S11*.

To further investigate inflammatory proteins mediating the effect of GlycA on incident MACE, we conducted mediation analysis using the proteomic data. Sixty-three proteins

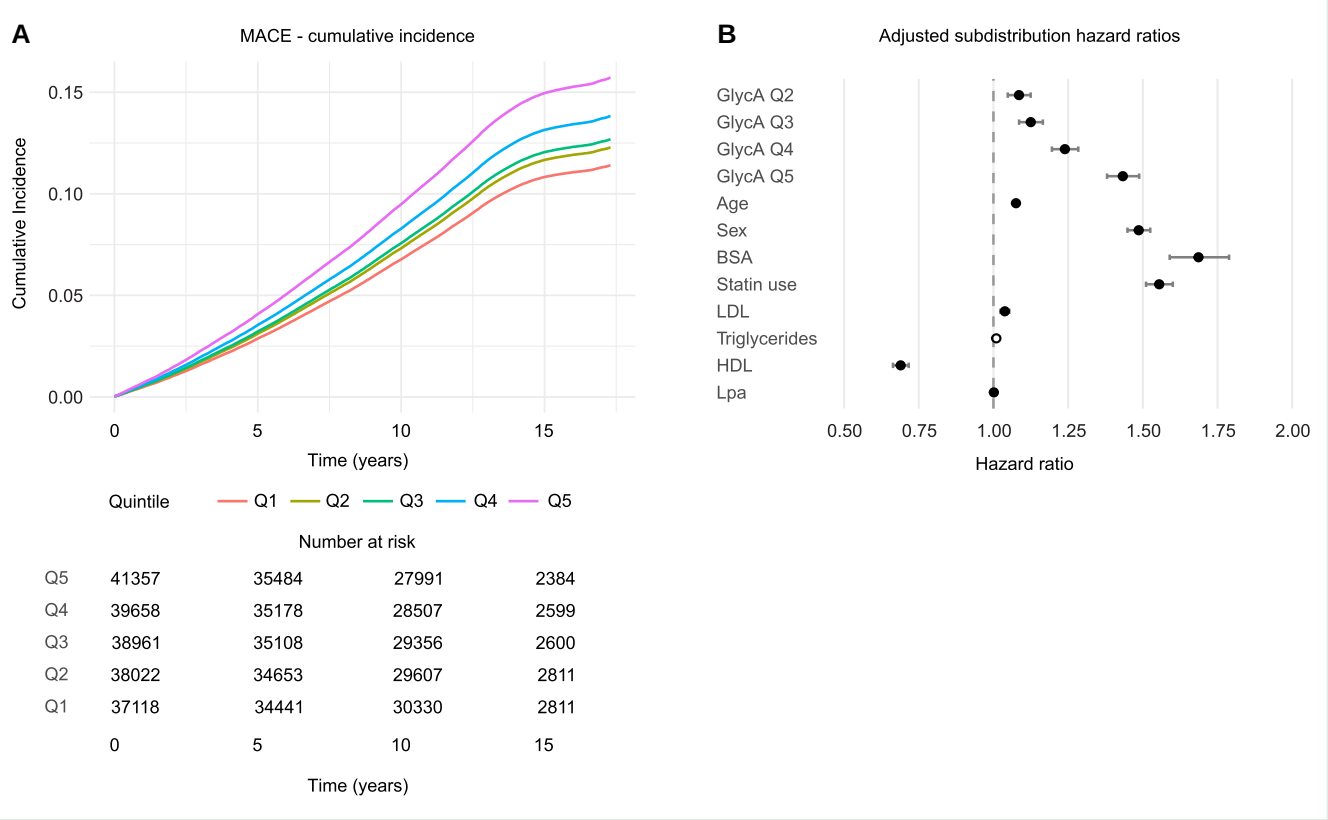


Figure 3. Cumulative incidence of first major cardiovascular events. *(A)* Covariate- and competing risk–adjusted cumulative incidence of first major cardiovascular events among initially healthy participants, stratified by quintiles of log-transformed and scaled GlycA levels. *(B)* Forest plot showing adjusted subdistribution hazard ratios from covariate- and competing risk–adjusted models across quintiles of baseline GlycA levels. Quintile 1 included the lowest biomarker levels and quintile 5 the highest levels. GlycA, glycoprotein acetyls; MACE, major adverse cardiovascular event

Downloaded from academic.oup.com/eurjpc/advance-article/doi/10.1093/eurjpc/zwag435/8802224 by Imperial College of Science Technology and Medicine user on 25 September 2026

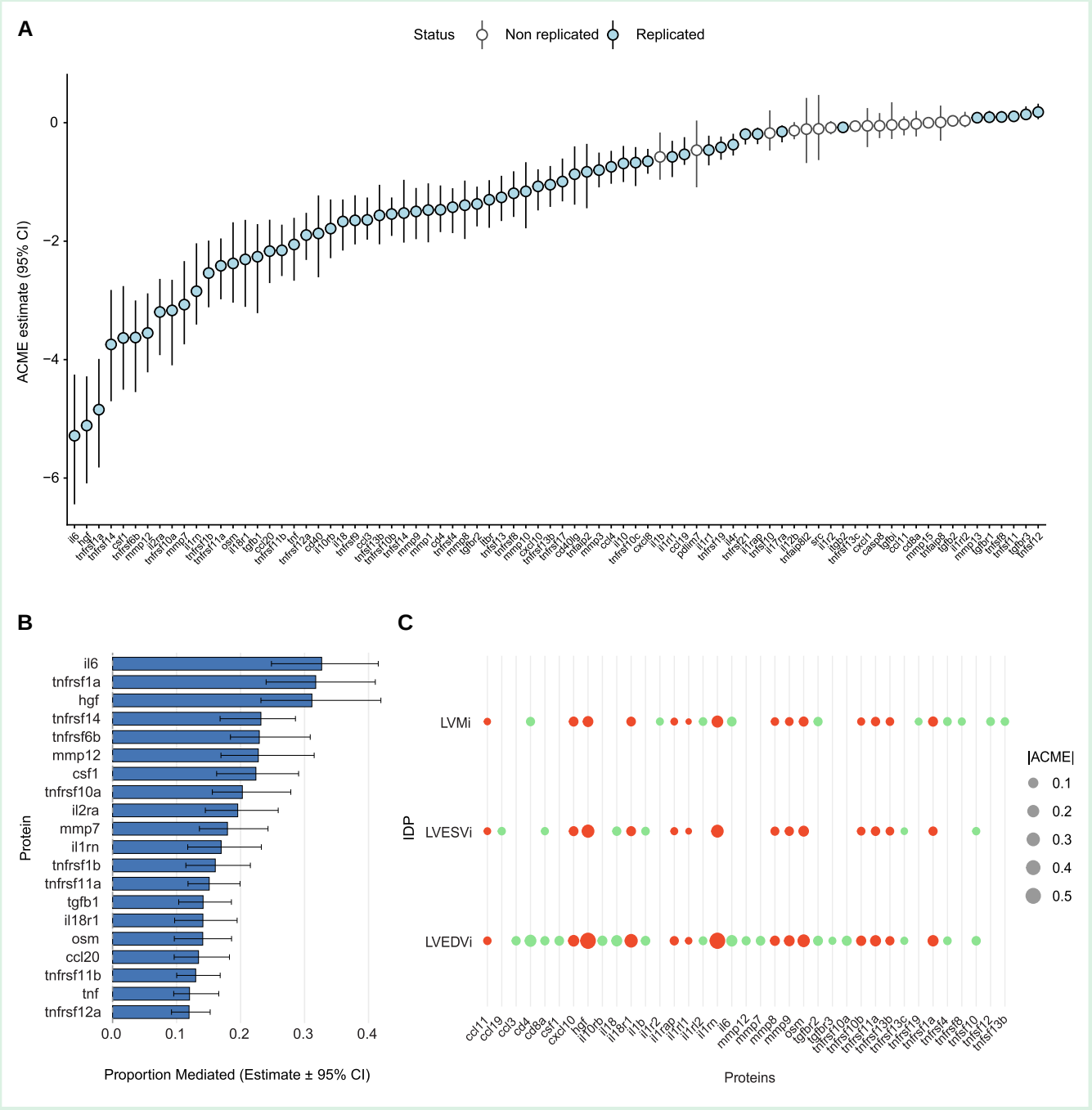


Figure 4. Proteins mediating the effect of inflammation on incident MACE. *(A)* Average causal mediation effect and corresponding 95% CI for each protein. Each model assessed one protein as a potential mediator of the association between log-transformed and scaled GlycA and incident MACE. A parametric survival model assuming a Weibull distribution was used, and models were adjusted for BSA, sex, age, age^2, the age–sex interaction, statin use, LDL cholesterol, triglycerides, HDL cholesterol, and Lp(a). Negative values indicate mediation of an association with shorter time-to-event. *(B)* Top 20 proteins with the highest proportion of mediated effect, representing the percentage of the total association between GlycA and incident MACE that is statistically mediated through each protein. *(C)* Proteins significantly mediating the effect of inflammation on survival and on LVEDVi, LVESVi, and LVMi. Red dots indicate proteins that replicated across all three IDPs and the survival analysis. Dots size is proportional to the absolute ACME value. ACME: average causal mediation effect; BSA, body surface area; HDL, high-density lipoprotein; LDL, low-density lipoprotein; Lp(a), lipoprotein a; IDP, imaging-derived phenotype; LVEDVi, left ventricle end-diastolic volume; LVESVi, left ventricle end-systolic volume; LVMi, left ventricle mass index; MACE, major adverse cardiovascular event

Downloaded from academic.oup.com/eurjpc/advance-article/doi/10.1093/eurjpc/zwag435/8802224 by Imperial College of Science Technology and Medicine user on 25 September 2026

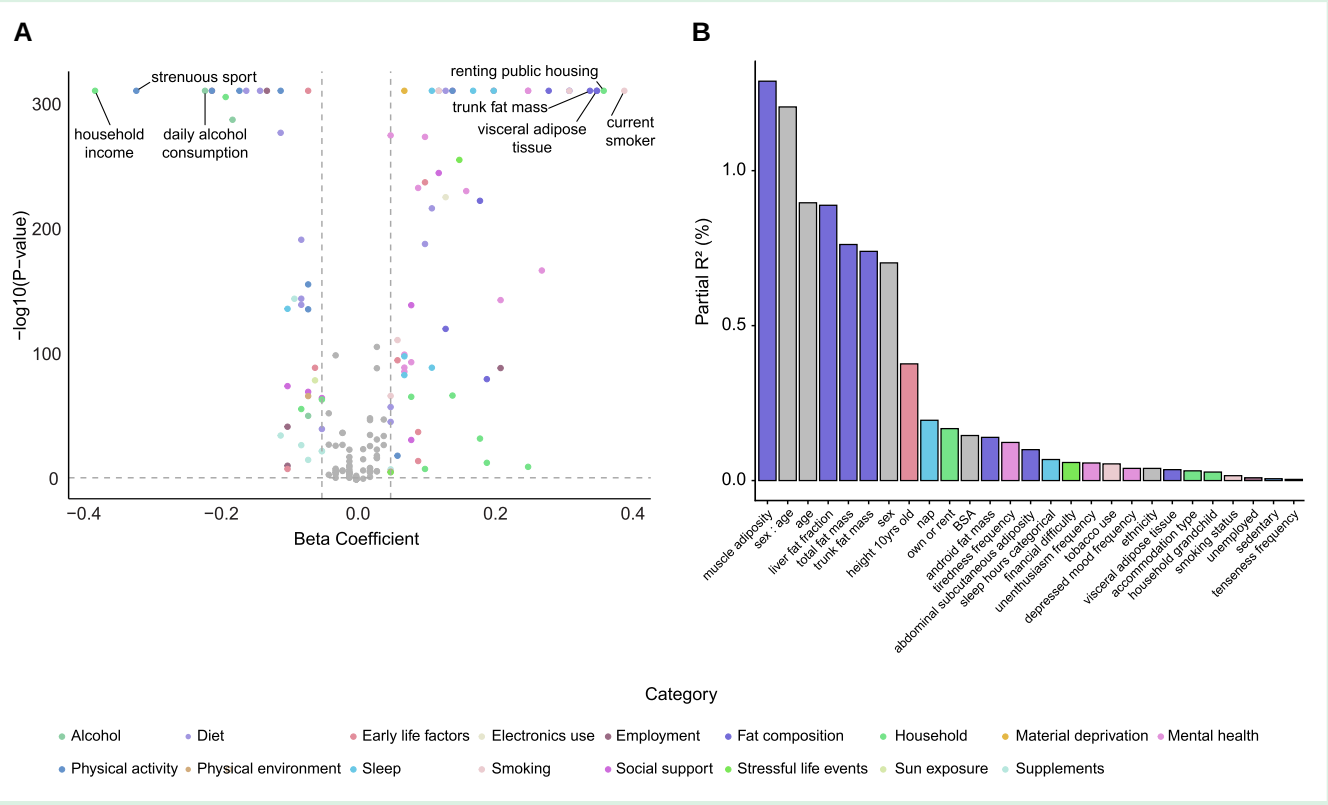


Figure 5. Exposome-wide association study. *(A)* Volcano plot showing the $-\log_{10}$ FDR-adjusted *P* value of the β coefficient for the association between each exposure (predictor) and log-transformed and scaled GlycA (outcome). Quantitative exposure variables were log-transformed and standardized. Models were adjusted for BSA, sex, age, age^2, age:sex interaction, and ethnicity. Grey dots indicate exposures with an absolute $\beta < 0.05$. Exposures with the largest absolute β values are labeled. *(B)* Bar plot showing the partial R^2 of each exposure, representing the proportion of GlycA variance explained by that exposure after adjustment for the other variables in the model. Results are shown for the 25 exposures with the largest absolute β coefficients from a multivariable linear model adjusted for BSA, sex, age, age^2, age interaction, and ethnicity. BSA, body surface area; FDR, false discovery rate; GlycA, glycoprotein acetyls

statistically mediated the association between GlycA and MACE (Figure 4), with the most significant ones mainly belonging to the TNF and IL-6 signalling pathways.

IL-6 exhibited the largest mediated effect of GlycA on incident MACE (ACME −5.28 [95% CI: −6.44 to −4.25, $P < 10^{-16}$]; proportion mediated 0.33 [95% CI: 0.25–0.41, $P < 10^{-16}$]), followed by HGF (ACME −5.11 [95% CI: −6.09 to −4.28, $P < 10^{-16}$]; proportion mediated 0.31 [95% CI: 0.23–0.42, $P < 10^{-16}$]). Notably, IL-1RA and HGF–both of which showed strong mediation effects on LV remodelling–also strongly mediated the association with the primary endpoint (Supplementary material online, *Files 16–17*). Figure 4C shows proteins that statistically mediate the association between GlycA, incident MACE, LV EDVi, LV ESVi, and indexed LV mass.

Exposures predicting inflammation

XWAS was conducted on 478 941 individuals with environmental factors and GlycA data available, and on 70 528 participants with available body fat composition measurements, testing 177 exposures in total (Supplementary material online, *File 18*). A total of 166 of 177 variables were significantly associated with GlycA levels (Figure 5A, Supplementary material online, *File 19*). Body fat composition, smoking status, psychological conditions, and low socioeconomic status showed the strongest associations with GlycA after adjusting for confounders. Total trunk fat mass ($\beta = 0.35$, $P < 10^{-50}$), current smoking status ($\beta = 0.39$, $P < 10^{-50}$), and renting from local authorities ($\beta = 0.36$, $P < 10^{-50}$)–a marker of low socioeconomic status–showed the strongest associations with inflammatory levels. Depressive symptoms, visceral fat, and android-distribution fat were also strongly positively associated with chronic inflammation. In contrast, variables reflecting higher socioeconomic status, physical activity, and healthier diet were negatively associated with GlycA levels.

When the 25 exposures most strongly associated with GlycA were included in a multivariable linear model together with confounders, the full model explained 18.6% of the variance in GlycA (Figure 5B, Supplementary material online, *File 20*). Adiposity-related measures explained the largest proportion of GlycA variance, including muscle adipose tissue infiltration (partial $R^2 = 1.3\%$), total fat mass (partial $R^2 = 0.8\%$), and trunk fat mass (partial $R^2 = 0.7\%$), followed by sleeping habits (daytime napping, partial $R^2 = 0.2\%$) and markers of socioeconomic deprivation (household ownership, partial $R^2 = 0.2\%$).

Downloaded from academic.oup.com/eurjpc/advance-article/doi/10.1093/eurjpc/zwag435/8802224 by Imperial College of Science Technology and Medicine user on 25 September 2026

No notable differences were observed in XWAS regression coefficients when analyses were performed separately by sex (Spearman correlation coefficient $r = 0.937$, $P < 10^{-50}$; Supplementary material online, *Figure S6A*, Supplementary material online, *Files 21–22*). Similarly, a strong correlation was observed between regression coefficients when hsCRP was used instead of GlycA as the predictor (Spearman correlation coefficient $r = 0.926$, $P < 10^{-50}$; Supplementary material online, *Figure S6B*, Supplementary material online, *File 23*).

Gene–environment interactions on inflammation

We investigated interactions between multi-ancestry PRSs and environmental factors in determining inflammatory levels in 485 717 individuals. We identified 101 exposure–PRS interactions that significantly modified the relationship between environmental factors (as predictors) and GlycA (as the outcome) after adjusting for the Townsend deprivation index–a marker of low socioeconomic status (Figure 6A, Supplementary material online, *Files 24–25*). Body fat composition, socioeconomic status, pollution, and mental health factors exhibited significant interactions with PRSs in determining GlycA levels (Supplementary material online, *Table S12*).

As an example, Supplementary material online, *Figure S7* shows Gly cA levels across strata of the Townsend deprivation index and PRS for cardiovascular disease. GlycA levels were significantly higher in the highest quartile of the exposure compared with the lowest ($P < 10^{-10}$). They also increased significantly between the first (lower risk) and fourth (higher risk) quartiles of PRS for cardiovascular disease across strata of the Townsend deprivation index.

We observed 49 exposure–PRS interactions that significantly affected the association between GlycA levels and MACE (Figure 6B, Supplementary material online, *Files 26–27*). Socioeconomic status, mental health, and physical activity emerged as the strongest exposure categories (Supplementary material online, *Table S13*).

Notably, 17 exposure–PRS interactions were replicated across both analyses (GlycA and MACE), predominantly involving socioeconomic variables. For instance, employment status significantly interacted with the CVD PRS, amplifying its effect on both GlycA ($\beta = 0.01$, $P = 0.02$) and MACE ($\beta = 1.07$, $P < 10^{-10}$).

Discussion

Our findings demonstrate that chronic systemic inflammation associates with cardiac remodelling characterized by reduced ventricular chamber volumes, diastolic impairment, and a compensatory chronotropic response. Circulating cytokines within IL-1 and TNF superfamilies emerged as key mediators of structural cardiac adaptation and adverse clinical outcomes. Elevated GlycA also independently predicted incident cardiovascular events and all-cause mortality beyond traditional risk factors and lipid levels. Additionally, we identified significant gene–environment interactions in which genetic susceptibility modified the inflammatory response to environmental exposures, suggesting that individual risk is determined by the convergence of inherited and acquired factors.

GlycA as a cardiovascular risk biomarker

We considered GlycA, an NMR spectroscopy-derived signal quantifying the circulating levels of multiple immunoregulatory proteins, as a marker of chronic inflammation. It has emerged as a stronger inflammatory biomarker compared with hsCRP,[28] as it reflects the activation of multiple biological pathways,[29] exhibits lower long-term intra-individual variability,[30] and is less sensitive to ethnicity, sex, and renal function.[31,32,33] GlycA has also been linked with incident CVD, making it an attractive systemic inflammatory biomarker for cardiovascular risk assessment.[12,34,35,36,37]

Our study represents the largest analysis to date, with long-term follow-up, assessing the relevance of GlycA as a cardiovascular risk factor. Specifically, we investigated the association between GlycA and adverse cardiac events in a large cohort of approximately 480 000 individuals, performing sensitivity analyses adjusting for potential confounders, established biomarkers, and competing risks. Our results support GlycA as an independent predictor of MACE. Although GlycA correlated with hsCRP, the addition of GlycA to a model including hsCRP and conventional cardiovascular risk factors significantly improved model fit and yielded a modest improvement in risk reclassification for 10-year prediction of MACE. These findings suggest that GlycA may capture aspects of chronic inflammation beyond those reflected by hsCRP, supporting its potential role as a complementary inflammatory biomarker.[38,39] However, further validation in prospective studies is needed to confirm its clinical utility.

Inflammation and cardiac remodelling

Systemic inflammation has been recognized as a key pathobiologic driver of the development, progression, and complications of many CVDs, including atherosclerosis, myocarditis, and HF.[40] Activation of inflammatory pathways has been implicated in the hemodynamic progression of heart failure with reduced ejection fraction (HFrEF) and heart failure with preserved ejection fraction (HFpEF).[16,41,42,43] While acute inflammation, assessed using hsCRP, has been linked to incident HF,[34] the pattern of remodelling that precedes overt disease and how this is mediated over time in the population by circulating factors is unknown.

Here, we investigated this relationship in a large community-living cohort with multi-omic profiling and CMR. We found that chronic inflammation was associated with ventricular volume reduction with relative wall thickening and mild diastolic impairment. The absence of atrial dilation suggests that filling pressures may not be chronically elevated. A modest increase in heart rate likely reflects physiological compensation for reduced stroke volumes. Although this pattern may be consistent with early inflammation-associated cardiac remodelling, alternative explanations such as differences in preload status, physical fitness, body composition, or subclinical comorbidities cannot be excluded. Considering that this phenotype is similar to that seen in uncomplicated diabetes,[44] we performed a sensitivity analysis excluding patients with prevalent diabetes and obesity, noticing a similar trend of inflammation-remodelling association.

Potential mechanisms of inflammasome-mediated remodelling include increased extracellular matrix deposition with up-regulation of collagen expression, as well as impaired calcium homeostasis and depressed myocyte contractility.[45] Future

Downloaded from academic.oup.com/eurjpc/advance-article/doi/10.1093/eurjpc/zwag435/8802224 by Imperial College of Science Technology and Medicine user on 25 September 2026

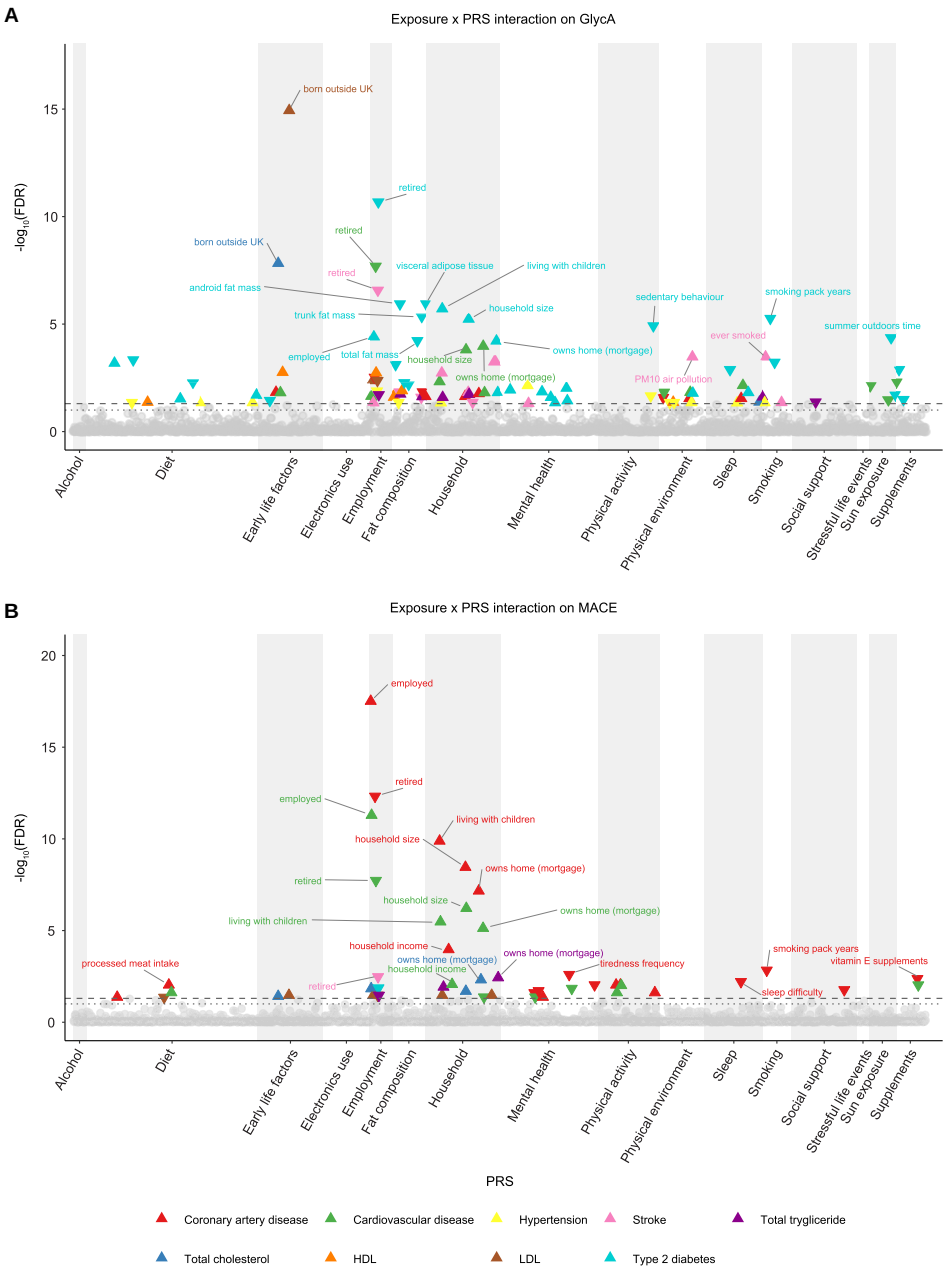


Figure 6. Exposure-gene interactions. *(A)* Manhattan plot showing the $-\log_{10}$ FDR-corrected *P* values of the interaction terms between exposures and PRS in predicting GlycA levels. Models were fitted with log-transformed and scaled GlycA as the dependent variable and exposures as independent variables. For each exposure, all PRS were tested in separate models by including a multiplicative interaction term, and models were adjusted for BSA, sex, age, age^2, age–sex interaction, ethnicity, and Townsend deprivation index. Triangles indicate interactions with an FDR-adjusted $P < 0.05$. Upward-pointing triangles indicate positive interaction effects ($\beta > 0$), suggesting that the association between the exposure and GlycA is stronger with increasing genetic risk, whereas downward-pointing triangles indicate negative interaction effects ($\beta < 0$), suggesting attenuation of the exposure effect with increasing genetic risk. The top 20 interactions are labeled. Non-significant interactions are shown as gray dots. *(B)* Manhattan plot showing the $-\log_{10}$ FDR-corrected *p*-values of the interaction terms between exposures and PRS in predicting incident MACE. For each exposure, all PRS were tested in separate models by including a multiplicative interaction term, and models were adjusted for BSA, sex, age, age^2, age–sex interaction, ethnicity, and Townsend deprivation index. Triangles indicate interactions with an FDR-adjusted $P < 0.05$. Upward-pointing triangles indicate positive interaction effects ($\beta > 1$), suggesting that the association between the exposure and MACE is stronger with increasing genetic risk, whereas downward-pointing triangles indicate negative interaction effects ($\beta < 1$), suggesting attenuation of the exposure effect with increasing genetic risk. The top 20 interactions are labeled. Non-significant interactions are shown as gray dots. FDR, false discovery rate; GlycA, glycoprotein acetyl; HDL, high-density lipoprotein; LDL, low density lipoprotein; MACE, major adverse cardiac event; PRS, polygenic risk score; UK; United Kingdom

Downloaded from academic.oup.com/eurjpc/advance-article/doi/10.1093/eurjpc/zwag435/8802224 by Imperial College of Science Technology and Medicine user on 25 September 2026

studies are needed to determine longitudinally whether sustained elevations in inflammatory biomarkers are associated with progression toward a restrictive hemodynamic phenotype and HFpEF.

Proteomic mediators as therapeutic targets

We investigated 80 circulating proteins, identifying 14 biomarker candidates associated with ventricular volume reduction and incident MACE, which were directly associated with GlycA and hsCRP levels. The most represented pathways involved the IL-1 and TNF superfamilies. IL-1RA, an endogenous inhibitor of IL-1α/β activity,[46,47] has been positively associated with cardiovascular risk in clinical and preclinical studies.[47,48] IL-1 blockade has significantly reduced the rate of recurrent cardiovascular events in patients with previous myocardial infarction,[49] though it has failed to improve outcomes in obese HFpEF patients.[50] However, IL-18, another IL-1 axis mediator and critical factor in so-called autoinflammatory IL-18opathies,[51] shows promise: receptor knockout mice exhibit attenuated LV dysfunction,[52,53] genetic variation appears to influence cardiovascular outcomes,[54,55] and pathway inhibition is currently being tested in clinical studies.[56,57]

Within the TNF superfamily, TNFrsf1A predicts HFpEF development and mortality,[58] although anti-cytokine therapy has not been successful in HFrEF trials.[59] TNFrsf11A (RANK/RANKL axis) and TNFrsf13B (B-cell immunity) are associated with CVD[60,61] and are therapeutic targets in other inflammatory conditions.[62,63] IL-6's association with MACE and LVEDVi is particularly relevant given the ongoing HERMES[64] and ZEUS[65] trials testing the effect of the monoclonal antibody ziltivekimab targeting residual inflammatory risk.[66] Additional mediators–HGF, matrix metalloproteinases 8 and 9, oncostatin M, and C-X-C motif chemokine ligand 10–represent further potential therapeutic targets emerging from our data.

Environmental exposures and genetic susceptibility

Our study provides the first large-scale systematic assessment of the relative contributions of environmental exposures and genetic susceptibility on chronic inflammation, as well as their interaction, in a population-based setting. Previous epidemiological studies have demonstrated robust associations between individual environmental and behavioral exposures and aging or mortality using exposome-wide approaches;[7] however, comparable comprehensive analyses focusing on inflammatory phenotypes have been lacking. In this context, the XWAS identifies smoking behavior, body fat composition, mental health, and socioeconomic status as the environmental factors most strongly associated with chronic inflammation.[67,68,69,70]

Beyond the main exposure effects, we systematically evaluated interactions between environmental exposures and polygenic risk for a range of CVDs, demonstrating that genetic susceptibility significantly modifies the relationship between environmental risk burden and inflammation. These findings indicate that individual inflammatory responses to environmental exposures are shaped by inherited risk and that polygenic scores for multiple CVDs may act through modulation of shared inflammatory pathways. Future work might examine whether combining polygenic risk assessment with biomarkers of chronic inflammation could predict susceptibility or resilience to inflammatory stressors and identify those most at risk of poor outcomes associated with modifiable cardiovascular risk factors and other environmental exposures.

Limitations

The UKB is a population-based cohort composed predominantly of individuals of White European ancestry and is known to be affected by healthy volunteer selection bias, with participants generally exhibiting more favorable socioeconomic and health characteristics than the general UK population.[71] The generalizability of our findings to other ethnic groups and higher-risk populations requires further investigation. In addition, the imaging sub-cohort represents a selected subset of UKB participants and may therefore be subject to additional selection bias. Nevertheless, previous studies have suggested that, despite limited representativeness, associations between exposures and outcomes observed in UKB are generally robust and broadly generalizable.[71] GlycA is assessed with NMR, which is not currently available in routine healthcare settings, and its predictive value compared with hsCRP needs to be validated in broader populations. Although a relatively large number of proteins were examined, they represent only a subset of the circulating proteome and do not necessarily capture intracellular or tissue-specific protein expression. Environmental exposures were measured with varying precision and do not capture the full complexity of the exposome, introducing potential measurement error and residual confounding. Multiple-testing correction reduces but does not eliminate the risk of false-positive findings, and independent replication remains necessary. Lastly, mediation analyses conducted in a cross-sectional setting should be viewed as exploratory and do not establish causal pathways, as residual confounding, reverse causation, and the lack of temporal separation between exposure, mediator, and outcome cannot be excluded.

Conclusions

These findings advance understanding of the role of chronic inflammation in heart disease, with IL-1 and TNF pathways implicated in adverse cardiac remodelling and cardiovascular risk, and exposure-gene interactions shaping individual susceptibility to systemic inflammation.

Supplementary Material

Supplementary material is available at *European Journal of Preventive Cardiology*

Author contributions

Conceptualization: M.C., D.O.R.; Methodology: M.C., D.O.R., S.T., K.R.; Formal analysis: M.C., L.H., S.K., P.G., J.Z., M.V.; Writing–original draft: M.C.; Writing–review and editing: L.H., S.K., L.C., D.O.R.; Visualization: M.C., D.O.R.; Supervision: D.O.R.; Project administration: D.O.R.; Funding acquisition: D.O.R.

Downloaded from academic.oup.com/eurjpc/advance-article/doi/10.1093/eurjpc/zwag435/8802224 by Imperial College of Science Technology and Medicine user on 25 September 2026

Funding

The study was supported by the Medical Research Council (MC_UP_1605/13); British Heart Foundation (RG/F/24/110138, RE/24/130023, CH/F/24/90015); and theNIHR Imperial Biomedical Research Centre. D.P.O'R. is also supported by the British Heart Foundation Big Beat Challenge award to CureHeart (BBC/F/21/220106).

Conflict of interest: D.P.O'R. has received fees from Bayer AG, and grant funding from Bayer AG and Calico Labs.

Data availability

Data from UK Biobank are available for approved research upon application from https://www.ukbiobank.ac.uk/enable-your-research/apply-for-access under the terms of the UK Biobank's data access policy.

References

1. Mensah GA, Arnold N, Prabhu SD, Ridker PM, Welty FK. Inflammation and cardiovascular disease: 2025 ACC scientific statement. *J Am Coll Cardiol* 2025 87:1381-1404. doi:10.1016/j.jacc.2025.08.047.
2. Alcaide P, Kallikourdis M, Emig R, Prabhu SD. Myocardial inflammation in heart failure with reduced and preserved ejection fraction. *Circ Res* 2024;**134**:1752–1766. doi:10.1161/CIRCRESAHA.124.323659.
3. Packer M. Differential pathophysiological mechanisms in heart failure with a reduced or preserved ejection fraction in diabetes. *JACC Heart Fail* 2021;**9**:535–549. doi:10.1016/j.jchf.2021.05.019.
4. Ridker PM, Moorthy MV, Cook NR, Rifai N, Lee IM, Buring JE. Inflammation, cholesterol, lipoprotein(a), and 30-year cardiovascular outcomes in women. *N Engl J Med* 2024;**391**:2087–2097. doi:10.1056/NEJMoa2405182.
5. Zacho J, Tybjaerg-Hansen A, Jensen JS, Grande P, Sillesen H, Nordestgaard BG. Genetically elevated C-reactive protein and ischemic vascular disease. *N Engl J Med* 2008;**359**:1897–1908. doi:10.1056/NEJMoa0707402.
6. Kurt B, Reugels M, Schneider KM, Zimmermann HW, Tacke F, Trautwein C, *et al.* C-reactive protein and cardiovascular risk in the general population. *Eur Heart J* 2025 47:1799-1810. doi:10.1093/eurheartj/ehaf937.
7. Argentieri MA, Amin N, Nevado-Holgado AJ, Sproviero W, Collister JA, Keestra SM, *et al.* Integrating the environmental and genetic architectures of aging and mortality. *Nat Med* 2025;**31**:1016–1025. doi:10.1038/s41591-024-03483-9.
8. Sanmarco LM, Chao CC, Wang YC, Kenison JE, Li Z, Rone JM, *et al.* Identification of environmental factors that promote intestinal inflammation. *Nature* 2022;**611**:801–809. doi:10.1038/s41586-022-05308-6.
9. Ong AD, Mann FD, Kubzansky LD. Cumulative social advantage is associated with slower epigenetic aging and lower systemic inflammation. *Brain Behav Immun Health* 2025;**48**:101096. doi:10.1016/j.bbih.2025.101096.
10. Gupta A, Shah K, Shukla A. Bridging traditional risk factors and genetic insights: a review on polygenic risk scores in cardiovascular diseases. *Adv Biomark Sci Technol* 2025;**7**:365–377. doi:10.1016/j.abst.2025.09.002.
11. Ritchie SC, Jiang X, Pennells L, Karthikeyan S, Xu Y, Danesh J, *et al.* Combined clinical, metabolomic, and polygenic scores for cardiovascular risk prediction. *Eur Heart J* 2025 47:1861-1873. doi:10.1093/eurheartj/ehaf947.
12. Chiesa ST, Charakida M, Georgiopoulos G, Roberts JD, Stafford SJ, Park C, *et al.* Glycoprotein acetyls: a novel inflammatory biomarker of early cardiovascular risk in the young. *J Am Heart Assoc* 2022;**11**:e024380. doi:10.1161/JAHA.121.024380.
13. Bycroft C, Freeman C, Petkova D, Band G, Elliott LT, Sharp K, *et al.* The UK Biobank resource with deep phenotyping and genomic data. *Nature* 2018;**562**:203–209. doi:10.1038/s41586-018-0579-z.
14. Zhang S, Wang Z, Wang Y, Zhu Y, Zhou Q, Jian X, *et al.* A metabolomic profile of biological aging in 250 341 individuals from the UK Biobank. *Nat Commun* 2024;**15**:8081. doi:10.1038/s41467-024-52310-9.
15. Bai W, Suzuki H, Qin C, Tarroni G, Oktay O, Matthews PM, *et al.* Recurrent neural networks for aortic image sequence segmentation with sparse annotations. In: *Medical Image Computing and Computer Assisted Intervention – MICCAI 2018*. 2018. p586–94. doi:10.1007/978-3-030-00937-3_67.
16. Sanders-van Wijk S, Tromp J, Beussink-Nelson L, Hage C, Svedlund S, Saraste A, *et al.* Proteomic evaluation of the comorbidity-inflammation paradigm in heart failure with preserved ejection fraction: results from the PROMIS-HFpEF study. *Circulation* 2020;**142**:2029–2044. doi:10.1161/CIRCULATIONAHA.120.045810.
17. Allen NE, Arnold M, Parish S, Hill M, Sheard S, Callen H, *et al.* Approaches to minimising the epidemiological impact of sources of systematic and random variation that may affect biochemistry assay data in UK Biobank. *Wellcome Open Res* 2021;**5**:222. doi:10.12688/wellcomeopenres.16171.2.
18. Julkunen H, Cichońska A, Slagboom PE, Würtz P. Metabolic biomarker profiling for identification of susceptibility to severe pneumonia and COVID-19 in the general population. *Elife* 2021;**10**:e63033. doi:10.7554/eLife.63033.
19. Petersen SE, Matthews PM, Francis JM, Robson MD, Zemrak F, Boubertakh R, *et al.* UK Biobank's cardiovascular magnetic resonance protocol. *J Cardiovasc Magn Reson* 2016;**18**:8. doi:10.1186/s12968-016-0227-4.
20. Bai W, Sinclair M, Tarroni G, Oktay O, Rajchl M, Vaillant G, *et al.* Automated cardiovascular magnetic resonance image analysis with fully convolutional networks. *J Cardiovasc Magn Reson* 2018;**20**:65. doi:10.1186/s12968-018-0471-x.
21. Puyol-Antón E, Ruijsink B, Bai W, Langet H, De Craene M, Schnabel JA, *et al.* Fully automated myocardial strain estimation from cine MRI using convolutional neural networks. In: *2018 IEEE 15th International Symposium on Biomedical Imaging (ISBI 2018)*. IEEE; 2018. p1139–1143. doi:10.1109/ISBI.2018.8363772.
22. Thanaj M, Mielke J, McGurk KA, Bai W, Savioli N, de Marvao A, *et al.* Genetic and environmental determinants of diastolic heart function. *Nat Cardiovasc Res* 2022;**1**:361–371. doi:10.1038/s44161-022-00048-2.
23. Bai W, Suzuki H, Huang J, Francis C, Wang S, Tarroni G, *et al.* A population-based phenome-wide association study of cardiac and aortic structure and function. *Nat Med* 2020;**26**:1654–1662. doi:10.1038/s41591-020-1009-y.
24. Windsor R, Jamaludin A, Kadir T, Zisserman A. Self-supervised multi-modal alignment for whole body medical imaging. arXiv:2107.06652. 2021. doi:10.48550/arXiv.2107.06652.
25. McCracken C, Raisi-Estabragh Z, Veldsman M, Raman B, Aung N, Fung K, *et al.* Multi-organ imaging demonstrates the heart-brain-liver axis in UK Biobank participants. *Nat Commun* 2022;**13**:7839. doi:10.1038/s41467-022-35321-2.
26. Benjamini Y, Hochberg Y. Controlling the false discovery rate: a practical and powerful approach to multiple testing. *J R Stat Soc Series B Stat Methodol* 1995;**57**:289–300. doi:10.1111/j.2517-6161.1995.tb02031.x.
27. Thompson DJ, Wells D, Selzam S, Peneva I, Moore R, Sharp K, *et al.* A systematic evaluation of the performance and properties of the UK Biobank polygenic risk score (PRS) release. *PLoS One* 2024;**19**:e0307270. doi:10.1371/journal.pone.0307270.
28. Lin JS, Evans CV, Johnson E, Redmond N, Coppola EL, Smith N. Nontraditional risk factors in cardiovascular disease risk assessment: updated evidence report and systematic review for the US preventive services task force. *JAMA* 2018;**320**:281–297. doi:10.1001/jama.2018.4242.
29. Ritchie SC, Würtz P, Nath AP, Abraham G, Havulinna AS, Fearnley LG, *et al.* The biomarker GlycA is associated with chronic inflammation and predicts long-term risk of severe infection. *Cell Syst* 2015;**1**:293–301. doi:10.1016/j.cels.2015.09.007.
30. Otvos JD, Shalaurova I, Wolak-Dinsmore J, Connelly MA, Mackey RH, Stein JH, *et al.* GlycA: a composite nuclear magnetic resonance biomarker of systemic inflammation. *Clin Chem* 2015;**61**:714–723. doi:10.1373/clinchem.2014.232918.
31. Gruppen EG, Riphagen IJ, Connelly MA, Otvos JD, Bakker SJL, Dullaart RPF. GlycA, a pro-inflammatory glycoprotein biomarker, and incident cardiovascular disease: relationship with C-reactive protein and renal function. *PLoS One* 2015;**10**:e0139057. doi:10.1371/journal.pone.0139057.
32. Seeling KS, Hehl L, Vell MS, Rendel MD, Creasy KT, Trautwein C, *et al.* Comorbidities, biomarkers and cause specific mortality in patients with irritable bowel syndrome: a phenome-wide association study. *United European Gastroenterol J* 2023;**11**:458–470. doi:10.1002/ueg2.12397.
33. Khera A, McGuire DK, Murphy SA, Stanek HG, Das SR, Vongpatanasin W, *et al.* Race and gender differences in C-reactive protein levels. *J Am Coll Cardiol* 2005;**46**:464–469. doi:10.1016/j.jacc.2005.04.051.
34. Jang S, Ogunmoroti O, Ndumele CE, Zhao D, Rao VN, Fashanu OE, *et al.* Association of the novel inflammatory marker GlycA and incident heart failure and its subtypes of preserved and reduced ejection fraction: the multi-ethnic study of atherosclerosis. *Circ Heart Fail* 2020;**13**:e007067. doi:10.1161/CIRCHEARTFAILURE.120.007067.
35. Puig-Jové C, Julve J, Castelblanco E, Julián MT, Amigó N, Andersen HU, *et al.* The novel inflammatory biomarker GlycA and triglyceride-rich lipoproteins are associated with the presence of subclinical myocardial dysfunction in subjects

Downloaded from academic.oup.com/eurjpc/advance-article/doi/10.1093/eurjpc/zwag435/8802224 by Imperial College of Science Technology and Medicine user on 25 September 2026

with type 1 diabetes mellitus. *Cardiovasc Diabetol* 2022;**21**:257. doi:10.1186/s12933-022-01652-z.
36. Akinkuolie AO, Buring JE, Ridker PM, Mora S. A novel protein glycan biomarker and future cardiovascular disease events. *J Am Heart Assoc* 2014;**3**:e001221. doi:10.1161/JAHA.114.001221.
37. Kraaijenhof JM, Nurmohamed NS, Nordestgaard AT, Verweij SL, Wareham NJ, Boekholdt SM, *et al.* Low-density lipoprotein cholesterol, C-reactive protein, and lipoprotein(a) universal one-time screening in primary prevention: the EPIC-Norfolk study. *Eur Heart J* 2025;**46**:3875–3884. doi:10.1093/eurheartj/ehaf209.
38. Ballout RA, Remaley AT. GlycA: a new biomarker for systemic inflammation and cardiovascular disease (CVD) risk assessment. *J Lab Precis Med* 2020;**5**:17. doi:10.21037/jlpm.2020.03.03.
39. Kasher M, Freidin MB, Williams FMK, Livshits G. CHARGE8 inflammation working group. GlycA and CRP are genetically correlated: insight into the genetic architecture of inflammageing. *Biomolecules* 2024;**14**:563. doi:10.3390/biom14050563.
40. Murphy SP, Kakkar R, McCarthy CP, Januzzi JL. Inflammation in heart failure: JACC state-of-the-art review. *J Am Coll Cardiol* 2020;**75**:1324–1340. doi:10.1016/j.jacc.2020.01.014.
41. Feng W, Li W. The study of ISO induced heart failure rat model. *Exp Mol Pathol* 2010;**88**:299–304. doi:10.1016/j.yexmp.2009.10.011.
42. Zhang L, Liebelt JJ, Madan N, Shan J, Taub CC. Comparison of predictors of heart failure with preserved versus reduced ejection fraction in a multiracial cohort of preclinical left ventricular diastolic dysfunction. *Am J Cardiol* 2017;**119**:1815–1820. doi:10.1016/j.amjcard.2017.03.005.
43. Yi A, Jian L, Xiaojing H, Hui X. The prevalence of th17 cells in patients with dilated cardiomyopathy. *Clin Invest Med* 2009;**32**:E144–E150. doi:10.25011/cim.v32i2.6032.
44. Jensen MT, Fung K, Aung N, Sanghvi MM, Chadalavada S, Paiva JM, *et al.* Changes in cardiac morphology and function in individuals with diabetes mellitus. *Circ Cardiovasc Imaging* 2019;**12**:e009476. doi:10.1161/CIRCIMAGING.119.009476.
45. Zhang H, Dhalla NS. The role of pro-inflammatory cytokines in the pathogenesis of cardiovascular disease. *Int J Mol Sci* 2024;**25**:1082. doi:10.3390/ijms25021082.
46. Toldo S, Abbate A. The role of the NLRP3 inflammasome and pyroptosis in cardiovascular diseases. *Nat Rev Cardiol* 2024;**21**:219–237. doi:10.1038/s41569-023-00946-3.
47. Herder C, de Las Heras Gala T, Carstensen-Kirberg M, Koenig W, Heier M, Krumsiek J, *et al.* Circulating levels of interleukin 1-receptor antagonist and risk of cardiovascular disease: meta-analysis of six population-based cohorts. *Arterioscler Thromb Vasc Biol* 2017;**37**:1222–1227. doi:10.1161/ATVBAHA.117.309307.
48. Vecile E, Dobrina A, Salloum FN, Van Tassell BW, Falcione A, Gustini E, *et al.* Intracellular function of interleukin-1 receptor antagonist in ischemic cardiomyocytes. *PLoS One* 2013;**8**:e53265. doi:10.1371/journal.pone.0053265.
49. Ridker PM, Everett BM, Thuren T, MacFadyen JG, Chang WH, Ballantyne C, *et al.* Antiinflammatory therapy with canakinumab for atherosclerotic disease. *N Engl J Med* 2017;**377**:1119–1131. doi:10.1056/NEJMoa1707914.
50. Van Tassell BW, Trankle CR, Canada JM, Carbone S, Buckley L, Kadariya D, *et al.* IL-1 blockade in patients with heart failure with preserved ejection fraction. *Circ Heart Fail* 2018;**11**:e005036. doi:10.1161/CIRCHEARTFAILURE.118.005036.
51. Landy E, Carol H, Ring A, Canna S. Biological and clinical roles of IL-18 in inflammatory diseases. *Nat Rev Rheumatol* 2024;**20**:33–47. doi:10.1038/s41584-023-01053-w.
52. Toldo S, Mezzaroma E, O'Brien L, Marchetti C, Seropian IM, Voelkel NF, *et al.* Interleukin-18 mediates interleukin-1-induced cardiac dysfunction. *Am J Physiol Heart Circ Physiol* 2014;**306**:H1025–H1031. doi:10.1152/ajpheart.00795.2013.
53. Carbone S, Lee PJH, Mauro AG, Mezzaroma E, De Nicolao A, Buzzetti R, *et al.* Interleukin-18 mediates cardiac dysfunction induced by western diet independent of obesity and hyperglycemia in the mouse. *Nutr Diabetes* 2017;**7**:e258. doi:10.1038/nutd.2017.1.
54. Tiret L, Godefroy T, Lubos E, Nicaud V, Tregouet DA, Barbaux S, *et al.* Genetic analysis of the interleukin-18 system highlights the role of the interleukin-18 gene in cardiovascular disease. *Circulation* 2005;**112**:643–650. doi:10.1161/CIRCULATIONAHA.104.519702.
55. Brennan SO, Kelly PJ, Gorey S, Lim WS, Harbison JA, McCabe DJH, *et al.* Genetically predicted IL-18 inhibition and risk of cardiovascular events: a Mendelian randomization study. *Circulation* 2025;**151**:334–336. doi:10.1161/CIRCULATIONAHA.124.072238.
56. Gabay C, Fautrel B, Rech J, Spertini F, Feist E, Schulze-Koops H, *et al.* Open-label, multicentre, dose-escalating phase II clinical trial on the safety and efficacy of tadekinig alfa (IL-18BP) in adult-onset still's disease. *Ann Rheum Dis* 2018;**77**:840–847. doi:10.1136/annrheumdis-2017-212608.
57. Nouri Barkestani M, Naserian S, Khoddam F, Shamdani S, Bambai B. Optimization of IL-1RA structure to achieve a smaller protein with a higher affinity to its receptor. *Sci Rep* 2022;**12**:7483. doi:10.1038/s41598-022-11100-3.
58. Marti CN, Khan H, Mann DL, Georgiopoulou VV, Yancy C, Dries DL, *et al.* Soluble tumor necrosis factor receptors and heart failure risk in older adults: health, aging, and body composition (health ABC) study. *Circ Heart Fail* 2014;**7**:5–11. doi:10.1161/CIRCHEARTFAILURE.113.000344.
59. Mann DL, McMurray JJV, Packer M, Swedberg K, Borer JS, Colucci WS, *et al.* Targeted anticytokine therapy in patients with chronic heart failure: results of the randomized etanercept worldwide evaluation (RENEWAL). *Circulation* 2004;**109**:1594–1602. doi:10.1161/01.CIR.0000124490.27666.B2.
60. Forde H, Davenport C, Harper E, Cummins P, Smith D. The role of OPG/RANKL in the pathogenesis of diabetic cardiovascular disease. *Cardiovasc Endocrinol Metab* 2018;**7**:28–33. doi:10.1097/XCE.0000000000000144.
61. Sage AP, Tsiantoulas D, Binder CJ, Mallat Z. The role of B cells in atherosclerosis. *Nat Rev Cardiol* 2019;**16**:180–196. doi:10.1038/s41569-018-0106-9.
62. Cummings SR, San Martin J, McClung MR, Siris ES, Eastell R, Reid IR, *et al.* Denosumab for prevention of fractures in postmenopausal women with osteoporosis. *N Engl J Med* 2009;**361**:756–765. doi:10.1056/NEJMoa0809493.
63. Navarra SV, Guzmán RM, Gallacher AE, Hall S, Levy RA, Jimenez RE, *et al.* Efficacy and safety of belimumab in patients with active systemic lupus erythematosus: a randomised, placebo-controlled, phase 3 trial. *Lancet* 2011;**377**:721–731. doi:10.1016/S0140-6736(10)61354-2.
64. Petrie M, Borlaug B, Buchholtz K, Chopra V, Dewan P, Ferreira JP, *et al.* HERMES: effects of Ziltivekimab versus placebo on morbidity and mortality in patients with heart failure with mildly reduced or preserved ejection fraction and systemic inflammation. *J Card Fail* 2024;**30**:126. doi:10.1016/j.cardfail.2023.10.024.
65. Ridker PM, Baeres FMM, Hveplund A, Koenig W, Libby P, Lüscher TF, *et al.* Rationale, design, and baseline clinical characteristics of the Ziltivekimab cardiovascular outcomes trial. *JAMA Cardiol* 2026;**11**:89–97. doi:10.1001/jamacardio.2025.4491.
66. May M. Eleven clinical trials that will shape medicine in 2026. *Nat Med* 2025;**31**:3943–3947. doi:10.1038/s41591-025-04083-x.
67. Berg AH, Scherer PE. Adipose tissue, inflammation, and cardiovascular disease. *Circ Res* 2005;**96**:939–949. doi:10.1161/01.RES.0000163635.62927.34.
68. Abohashem S, Saeed F, Münzel T, Osborne MT, Shin LM, Tawakol A, *et al.* Imaging findings associated with socioenvironmental exposures inform mechanisms of cardiovascular disease. *Arterioscler Thromb Vasc Biol* 2025;**45**:2164–2178. doi:10.1161/ATVBAHA.125.322470.
69. Abohashem S, Qamar I, Grewal SS, Gharios C, Osborne MT, Shin LM, *et al.* Depression and anxiety associate with adverse cardiovascular events via neural, autonomic, and inflammatory pathways. *Circ Cardiovasc Imaging* 2025;**19**:e017706. doi:10.1161/CIRCIMAGING.124.017706.
70. Ma Y, Zhang J, Li D, Tang L, Li Y, Cui F, *et al.* Genetic susceptibility modifies relationships between air pollutants and stroke risk: a large cohort study. *Stroke* 2024;**55**:113–121. doi:10.1161/STROKEAHA.123.044284.
71. Fry A, Littlejohns TJ, Sudlow C, Doherty N, Adamska L, Sprosen T, *et al.* Comparison of sociodemographic and health-related characteristics of UK Biobank participants with those of the general population. *Am J Epidemiol* 2017;**186**:1026–1034. doi:10.1093/aje/kwx246.

Downloaded from academic.oup.com/eurjpc/advance-article/doi/10.1093/eurjpc/zwag435/8802224 by Imperial College of Science Technology and Medicine user on 25 September 2026